Genome-wide screen for deficiencies modifying *Cyclin G*-induced developmental instability in *Drosophila melanogaster*

Valérie Ribeiro[1], Marco Da Costa[1], Delphine Dardalhon-Cuménal [1], Camille A. Dupont[1], Jean-Michel Gibert[1], Emmanuèle Mouchel-Vielh[1], Hélène Thomassin[1], Neel B. Randsholt[1], Vincent Debat[3*] and Frédérique Peronnet[1*]

[1] Sorbonne Université, CNRS, Inserm, Développement Adaptation et Vieillissement, Dev2A, F75005 Paris, France

[2] Sorbonne Université, CNRS, Inserm, Institut de Biologie Paris-Seine, IBPS, F75005 Paris, France

[3] Institut de Systématique, Evolution, Biodiversité (ISYEB), Muséum national d'Histoire naturelle, CNRS, Sorbonne Université, EPHE, Université des Antilles CP 50, 57 rue Cuvier, 75005 Paris, France

*** Correspondence:**
Co-last and co-corresponding Author
frederique.peronnet@sorbonne-universite.fr
vincent.debat@mnhn.fr

Keywords: developmental instability, Drosophila, fluctuating asymmetry (FA), Cyclin G, genetic screen.

ABSTRACT

In spite of long-lasting interest and research efforts, the genetic bases of developmental stability – the robustness to developmental noise – and its most commonly used estimator, fluctuating asymmetry (FA), remain poorly understood. The *Drosophila melanogaster Cyclin G* gene (*CycG*) encodes a transcriptional cyclin that regulates growth and the cell cycle. Over-expression of a potentially more stable isoform of the protein (deleted of a PEST-rich domain, hereafter called $CycG^{\Delta P}$) induces extreme wing size and shape FA (*i.e.* high

31 developmental noise), indicating a major disruption of developmental stability. Previous
32 attempts to identify the genetic bases of FA have been impeded by developmental stability
33 itself, *i.e.* by the constitutively low level of developmental noise, strongly limiting the power to
34 detect any effect. Here, we leverage the extreme developmental instability induced by the
35 overexpression of *CycG*$^{\Delta P}$, to explore the genetic bases of FA with a considerably enhanced
36 power: we use this genetic context to perform a genome-wide screen for deficiencies that
37 enhance or reduce *CycG*$^{\Delta P}$-induced wing FA. 499 deficiencies uncovering about 90% of the
38 euchromatic genome were combined with a recombinant chromosome expressing *CycG*$^{\Delta P}$.
39 We identified 13 and 16 deficiencies that enhance and decrease FA, respectively. Analysis
40 of mutants for some genes located in these deficiencies shows that Cyclin G ensures
41 homogeneous growth of organs in synergy with the major morphogens of the wing, Dpp and
42 Wg, as well as the Hippo and InR/TOR pathways. They also reveal that *CycG*$^{\Delta P}$-induced FA
43 involves Larp, a potential direct interactor of Cyclin G, that regulates translation at the
44 mitochondrial membrane. This opens up new research perspectives for understanding
45 developmental stability, suggesting a significant role for mitochondrial activity in this process.

46 **INTRODUCTION**

47

48 Developmental noise results from the inherent variability of biological processes, that
49 operates independently of genetic or environmental factors (for a review on concepts see 1).
50 Developmental stability refers to the buffering of developmental noise. In bilaterians, an
51 estimate of developmental noise is provided by fluctuating asymmetry (FA), which refers to
52 slight, random deviations from perfect symmetry in paired structures, such as bilateral organs.
53 The genetic bases of developmental stability remain largely unknown. Investigation of
54 mandible size and shape FA in a population of mice has identified a few single-locus
55 Quantitative Loci Traits (QTLs) (2). In *Drosophila*, the wings, which have a highly stereotyped
56 organisation, are commonly used to measure FA, the variance in the difference between the
57 left and right wing in a population. Genome-wide deficiency mapping of regions responsible
58 for developmental noise has identified deficiencies associated with increased centroid size or
59 shape FA (3,4). However, the consistently low level of developmental noise - which greatly
60 limits the ability to detect any effects - likely explains why no attempts have been made to
61 identify the genes responsible for these effects within the QTLs or deficiencies.

62 In *Drosophila melanogaster,* the *Cyclin G* gene (*CycG*), which encodes a
63 transcriptional cyclin, has been implicated in developmental noise (5,6). Indeed,
64 overexpression of $CycG^{\Delta P}$, a modified version of Cyclin G that lacks the C-terminal PEST
65 domain and is therefore potentially more stable, induces an unprecedented high level of size
66 and shape FA (40-fold increase compared to control). The strongly destabilized system
67 induced by $CycG^{\Delta P}$ overexpression offers a unique opportunity to investigate the genetic
68 bases of developmental stability. In this study we used $CycG^{\Delta P}$ overexpression to perform a
69 genome-wide screen for deficiencies that enhance or reduce $CycG^{\Delta P}$-induced wing size FA.
70 495 deficiencies uncovering about 90% of the euchromatic genome were combined with a
71 recombinant chromosome expressing $CycG^{\Delta P}$. We thus identified 13 deficiencies that
72 enhance FA and 16 deficiencies that decrease it. Analysis of mutants for some genes located
73 in these deficiencies shows that Cyclin G ensures homogeneous growth of organs in synergy
74 with morphogens and growth control pathways. They also suggest an impact of mitochondrial
75 activity on developmental stability.

76

77 **MATERIAL AND METHODS**

78

79 **Genetics**

80 Flies were raised in yeast-cornflour broth (yeast extract 75 g/L, cornflour 90 g/L, agar-
81 agar 10.7 g/L, methyl 4-hydroxybenzoate 5.5 g/L) at 25°C. Lines carrying deficiencies (*Df*)
82 were obtained from the Bloomington stock center (Supplementary Table 1). These lines have
83 been generated in two different w^{1118} genetic backgrounds (stocks BL-5905 and BL-6326)
84 that were used as negative controls (further called w^{5905} and w^{6326}, respectively). The mutant
85 alleles used in this study are listed in Supplementary Table 2. The *da-Gal4,UAS-CycG*$^{\Delta P}$ third
86 chromosome, obtained by genetic recombination (5), was used as a positive control. Due to
87 high lethality and low fertility, this chromosome was maintained against the *TM6c,Sb*
88 balancer, in males, at 18°C.

89 In order to address the genetic interactions between *CycG* and each deficiency, 5
90 replicate crosses containing 6 deficiency or control females and 5 *da-Gal4*, *UAS-*
91 *CycG*$^{\Delta P}$*/TM6c, Sb* or *da-Gal4* males were performed. Series of experiments with up to 25
92 deficiencies were performed, each series including the appropriate positive and negative
93 controls. Care was taken to keep the crosses in standardized conditions: tubes used for a
94 given series were from the same batch, they were maintained at 25°C on the same incubator
95 floor, parents were transferred into new tubes each 48 h, three times, then discarded. The
96 offspring was counted and kept in 70 % ethanol. Thirty females of the desired genotype
97 (*Df*/*da-Gal4*, *UAS-CycG*$^{\Delta P}$, +/*da-Gal4*, *UAS-CycG*$^{\Delta P}$, *Df/da-Gal4* or *+/da-Gal4*) were
98 randomly sampled (Supplementary Figure 1).

99

100 **Measurements and statistical analysis**

101 The wings were mounted and scanned as described (5). The distance between
102 landmarks 3 and 13 was used to estimate wing length (5) (Supplementary Figure 1). Each
103 measurement was taken twice. Genetic interactions between individual genes and *CycG*$^{\Delta P}$
104 were tested using the same protocol.

105 FA of wing length was estimated using the FA10 index as previously described (5).
106 The nortest package was used to test normality of the difference between left- and right-wing
107 size (Shapiro-Wilk and Lilliefors tests) as well as skewness and kurtosis. The rare outliers
108 that perturbated normality, skewness (< -0.5 or > +0.5) or kurtosis (< -3 or > +3) were
109 eliminated from the sample (see number of individuals in Supplementary Table 3). F-tests
110 were performed to compare FA of the assays to the one of the series internal controls (*Df*/*da-*
111 *Gal4*, *UAS-CycG*$^{\Delta P}$ compared to +/*da-Gal4*, *UAS-CycG*$^{\Delta P}$, *Df/da-Gal4* compared to *+/da-*

112 *Gal4*). Holm-Bonferroni correction was applied to each series. Inter-individual variance of
113 wing length represented the variance of the individual mean wing length in the same
114 population.
115
116 **RESULTS**
117 **Genome-wide screen for deficiencies that modify *CycG*-induced fluctuating**
118 **asymmetry**
119 To scan the whole genome for modification of *CycG*$^{\Delta P}$-induced FA, we used a set of 499
120 deficiencies uncovering approximately 90% of the euchromatic genome (Supplementary
121 Table 1). Of these, 4 deficiencies were too weak to be crossed (Supplementary Table 1). A
122 primary screen was performed by crossing females of the remaining 495 deficiencies with *da-*
123 *Gal4*, *UAS-CycG*$^{\Delta P}$*/TM6c, Sb* males (Supplementary Figure 1). As the FA values varied from
124 experiment to experiment, a positive control (*w* females crossed with *da-Gal4*, *UAS-*
125 *CycG*$^{\Delta P}$*/TM6c,Sb* males) and a negative control (*w* females crossed with *da-Gal4/TM6c,Sb*
126 males) were systematically included in each experimental series to serve as intrinsic
127 standards. Forty-one deficiencies were lethal or sub-lethal when combined with the *da-*
128 *Gal4*, *UAS-CycG*$^{\Delta P}$ chromosome, preventing FA analyses (Supplementary Table 1). Two
129 deficiencies produced damaged wings when combined with *da-Gal4*, *UAS-CycG*$^{\Delta P}$, rendered
130 them unmeasurable (Supplementary Table 1). A total of 16,200 fly wings were mounted and
131 analysed in this primary screen. Of the 452 deficiencies whose combination with *da-*
132 *Gal4*, *UAS-CycG*$^{\Delta P}$ produced viable flies with usable wings, most did not modify *CycG*$^{\Delta P}$-
133 induced FA (neutral deficiencies). However, 39 deficiencies and 21 significantly decreased or
134 increased *CycG*$^{\Delta P}$-induced FA, respectively (Supplementary Table 1). We then performed a
135 secondary screen by crossing females of these 60 deficiencies with *da-Gal4*, *UAS-*
136 *CycG*$^{\Delta P}$*/TM6c,Sb* or *da-Gal4* males in order to replicate the primary screen while measuring
137 the FA of the deficiencies independently of *CycG*$^{\Delta P}$ overexpression. In addition, 8 neutral
138 deficiencies were randomly selected to confirm the absence of an effect. The results of this
139 secondary screen – a total of 4640 fly wings were mounted and analysed – are shown in
140 Supplementary Table 3. Of the 68 deficiencies tested, only three, *Df(2L)BSC17*,
141 *Df(1)BSC582*, and *Df(3L)BSC419*, increased FA when combined with *da-Gal4* in absence of
142 *CycG*$^{\Delta P}$ expression. None decreased it. Nevertheless, the increase was rather modest
143 compared to that observed in context of *CycG*$^{\Delta P}$ expression (3.3, 3.4 and 4.8 *versus* 28.5,
144 73.4 and 73.4 for the intrinsic positive controls, respectively). Interestingly,

145 *Df(3L)BSC419* partially overlaps *Df(3L)ED4978*, which has already been shown to increase
146 wing shape and bristle FA (3,4). The absence of *CycG*$^{\Delta P}$-induced FA modification was verified
147 for the 8 neutral deficiencies. However, the secondary screen eliminated some deficiencies
148 whose effect on *CycG*$^{\Delta P}$-induced FA was no longer significant, probably due to the variability
149 of the internal control. Thus, the screen ended with 29 modifier deficiencies: 16 that
150 reproducibly decreased *CycG*$^{\Delta P}$-induced FA and 13 that reproducibly enhanced it, further
151 referred to as decreasing (D) and enhancing (E) deficiencies, respectively (Table 1 and Figure
152 1). We did not observe any significant correlation between the size of these deficiencies and
153 the amplitude of their effect on *CycG*$^{\Delta P}$-induced FA (Figure 2A).

154 Surprisingly, the 13 E deficiencies clustered on the second chromosome and the left
155 arm of the third chromosome whereas the 16 D deficiencies clustered on the X chromosome
156 and the right arm of the third chromosome (Table 1). The mean wing size of all *Df; da-*
157 *Gal4*, *UAS-CycG*$^{\Delta P}$ flies was smaller than that of *Df; da-Gal4* flies, indicating that *CycG*$^{\Delta P}$
158 expression had a dominant effect on size reduction (Figure 2B and Supplementary Figure 2).
159 Lastly, we observed a positive correlation between FA and inter-individual variance (Figure
160 2C). As environmental conditions cannot be fully controlled and individuals are not genetically
161 perfectly identical, this inter-individual variance thus reflects minute genetic and
162 environmental differences. Whether organisms are simultaneously robust to developmental
163 noise, environmental and genetic effects is unclear. This positive correlation between FA and
164 inter-individual variance suggests a match between developmental stability and
165 environmental/genetic robustness.

166 Taken together, these results confirmed that *CycG*$^{\Delta P}$ expression strongly perturbs
167 developmental stability. In addition, we identified 29 deficiencies among the 452 analysed
168 that enhanced or decreased *CycG*$^{\Delta P}$-induced FA and could thus contain genes important for
169 developmental stability. These genes could therefore be partners of *CycG* in the mechanisms
170 that maintain developmental stability.

171

172 **Identification of genes that modify *CycG*$^{\Delta P}$-induced fluctuating asymmetry**

173 We next set out to identify partners of *CycG* in developmental stability within these
174 deficiencies. Interestingly, *Df(3R)ED6361*, which uncovers *CycG*, reduced the FA induced by
175 *CycG*$^{\Delta P}$ expression, suggesting that expression of *CycG*$^{\Delta P}$ behaved as a dominant negative
176 mutant and that the deviation from symmetry it induced was dose-dependent. Taken together,
177 the E deficiencies contained 736 genes (576 protein-coding genes and 160 non-protein-

178 coding genes), and the D deficiencies 865 genes (715 protein-coding genes and 150 non-
179 protein-coding genes), making it impossible to test mutants of these genes individually. To
180 select which mutants to test, we focused on genes encoding direct protein partners of
181 Cyclin G or genes involved in the control of growth (Supplementary Table 2).

182 Although located in D deficiencies (Supplementary Table 3), mutants or RNAi lines for
183 *Aladin* (7), *CG9426* (FBgn0032485), *E5* (8), *eEF2* (9), and *SAK* (10) which encode direct
184 Cyclin G physical interactors, significantly increased *CycG*$^{\Delta P}$-induced FA (Figure 3). Other
185 genes, or combinations of genes, in these deficiencies may be responsible for the observed
186 effects. On the other hand, two RNAi lines for *larp*, which is located in a D deficiency
187 (*Df(3R)BSC322*) and also encodes a direct Cyclin G physical interactor (11), significantly
188 reduced *CycG*$^{\Delta P}$-induced FA (Figure 3). Larp and Cyclin G may thus be direct partners in a
189 process important for developmental stability.

190 The Hippo signalling pathway plays a key role in controlling organ size (10). *Merlin*
191 (*Mer*), which encodes a positive regulator of this pathway that interacts directly with Cyclin G
192 (11), is located in the D deficiency *Df(1)BSC871*. Additionally, *hippo* (*hpo*), which encodes
193 the kinase of the pathway, is located in *Df(2R)ED3728*, which increased *CycG*$^{\Delta P}$-induced FA.
194 This prompted us to investigate the impact of other members of the Hippo pathway on
195 *CycG*$^{\Delta P}$-induced FA. Mutants for *Mer, hpo, ft*, *exp*, *wts* and *ban*, significantly increased it
196 (Figure 4A). Furthermore, *Mer* inactivation also increased FA independently of *CycG*
197 deregulation (Figure 4A). These results suggest that the Hippo pathway plays a role in
198 developmental stability.

199 The *mTor* gene, which encodes the central member of another key regulator of growth
200 (11), the InsulinR/TOR signalling pathway (InR/TOR) belongs to a deficiency that reduced
201 *CycG*$^{\Delta P}$-induced FA [*Df(2L)BSC277*]. Furthermore, Cyclin G interacts directly with three
202 actors of this pathway : Akt1, PP2A and Wdb (12,13). We thus tested the effect of *mTor* and
203 other members of the pathway for their effect on *CycG*$^{\Delta P}$-induced FA. Most of these,
204 particularly mutants for *Akt1*, *S6K*, *foxo*, *PTEN*, *mTor* and *wdb*, increased *CycG*$^{\Delta P}$-induced
205 FA. This suggests that the interaction between Cyclin G and the InR/TOR pathway is crucial
206 for developmental stability (Figure 4B).

207 Finally, two major morphogens of the wing, *dpp* and *wg* [for a review see (14)],
208 belonged to deficiencies that enhanced *CycG*$^{\Delta P}$-induced FA [*Df(2L)Exel7011* and
209 *Df(2L)BSC291*, respectively]. Mutants for both genes also increased *CycG*$^{\Delta P}$-induced FA,
210 indicating that we had identified at least one gene responsible for this effect within each

211 deficiency (Figure 4C).

212

213 **DISCUSSION**

214

215 In our efforts to identify deficiencies that modify *CycG*$^{\Delta P}$-induced FA, we found that 13
216 deficiencies out of 452 enhanced it (E deficiencies) while 16 deficiencies decreased it (D
217 deficiencies). Notably, these deficiencies were not evenly distributed across all
218 chromosomes. The D deficiencies were enriched on chromosomes X and 3R, whereas the E
219 deficiencies were concentrated on chromosomes 2 and 3L. This pattern suggests that
220 chromosomes 2 and 3L may have a general positive effect on developmental stability. In
221 addition, we observed that the vast majority of modifier deficiencies (65 out of the 68 tested)
222 does not affect FA on their own. Finally, the 13 deficiencies that enhance *CycG*$^{\Delta P}$-induced FA
223 represent only 4.1 % of the *Drosophila melanogaster* genome. Collectively, these results
224 indicate that under normal rearing conditions the control of growth is highly robust.
225 Overexpression of *CycG*$^{\Delta P}$ using the Gal4/UAS system provides an entry point to
226 discover genes and gene networks that are essential for growth homeostasis. Not
227 surprisingly, we found that the major morphogens (Dpp and Wg) and growth pathways
228 (InR/Tor and Hippo pathways) are essential for developmental stability. In line with our
229 findings, alternative splicing of *yki*, which encodes the transcription factor Yorkie, a target of
230 the Hippo pathway, has previously been shown to contribute to developmental stability (15).
231 Furthermore, Merlin that promotes assembly of a functional Hippo signaling complex at the
232 apical cell cortex has been shown to directly interact with Cyclin G (12). Beyond its specific
233 role, Cyclin G may be unique in that it sits at the crossroads of many signalling pathways. Our
234 previous systems biology approach has indeed shown that *CycG* is linked to many genes in
235 the wing imaginal disc (16). These new findings confirm that *CycG* may be a hub within a
236 complex genetic network important for the robustness of organ growth. We have previously
237 shown that expression of *CycG*$^{\Delta P}$ abolishes the strong negative correlation between cell size
238 and cell number observed in wild-type fly wings (5). Cyclin G may orchestrate growth
239 homeostasis by ensuring the proper coordination of growth and the cell cycle, which would
240 be critical for developmental stability. This central role may explain the spectacular effects of
241 its deregulation on fluctuating asymmetry.

242 Some potential direct Cyclin G partners are included in the deficiencies that modify
243 *CycG$^{\Delta P}$*-induced FA. Strikingly, these partners belong to different gene ontology categories,
244 ranging from the aforementioned Merlin to transcription factors (*e.g.* E5), translation
245 regulators (*e.g.* Larp) and proteins involved in protein degradation (*e.g.* Cul2), reinforcing the
246 idea that Cyclin G may be involved in diverse cellular processes. Among the genes encoding
247 these potential direct partners, *larp* is the only one whose inactivation strongly reduces
248 *CycG$^{\Delta P}$*-induced FA, suggesting that the effect of Cyclin G on FA requires this direct
249 interaction. *Larp* encodes an evolutionarily conserved RNA-binding protein that forms a
250 complex with the Poly(A) binding protein (PABP), a translation regulator (17,18). In addition,
251 Larp recognises mRNAs with a 5' Terminal OligoPyrimidine (5' TOP) motif, *i.e.* mRNAs
252 encoding proteins essential for protein synthesis such as ribosomal proteins or translation
253 factors (19). More recently, Larp has been shown to play a dual role as a translational
254 repressor and a stabiliser of 5' TOP mRNAs (20). In particular, when phosphorylated by
255 Pink1, Larp inhibits translation at the mitochondrial outer membrane suggesting that it may
256 have an effect on the production of new mitochondria(21). Interestingly, in wing imaginal discs
257 expressing *CycG$^{\Delta P}$*, genes involved in translation are up-regulated and those involved in
258 metabolism and mitochondrial activity are down-regulated (16). Taken together, these data
259 support the idea that there may be a link between developmental stability and the regulation
260 of mitochondrial activity.

261

262 **FIGURES**

263

264 **Figure 1: Secondary screen – Analysis of the 60 candidate deficiencies isolated from**
265 **the primary screen.**

266 **A –** FA of 39 deficiencies that decreased *CycG$^{\Delta P}$*-induced FA in the primary screen
267 normalised to the FA of *da-Gal4, UAS-CycG$^{\Delta P}$* (red line). 16 of them reproduced the results
268 of the primary screen (orange).

269 **B –** FA of 21 deficiencies that enhanced *CycG$^{\Delta P}$*-induced FA in the primary screen normalised
270 to the FA of *da-Gal4, UAS-CycG$^{\Delta P}$* (red line). 13 of them reproduced the results of the primary
271 screen (green).

272 *p<0.05, **p<0.01, ***p<0.001

Figure 2: Secondary screen - Relationship between fluctuating asymmetry and deficiency length, mean wing size and inter-individual variance.

A – FA (fold change) of the 16 decreasing (D) deficiencies (orange), the 13 enhancing (E) deficiencies (green) and 8 neutral deficiencies (grey) versus deficiency length. No significant correlation was observed between the two parameters (Pearson coefficient, R= -0.15).

B - FA of the 16 decreasing (D) deficiencies (orange) and the 13 enhancing (E) deficiencies (green) combined with *da-Gal4, UAS-CycG$^{\Delta P}$* (filled circles) or not (empty circles) versus mean wing size. Filled grey square: *+/da-Gal4, UAS-CycG$^{\Delta P}$*; empty grey square: *+/da-Gal4*. A strong negative correlation was observed between these parameters (R= -0.65).

C – FA (log10) of the 16 decreasing (D) deficiencies (orange) and the 13 enhancing (E) deficiencies (green) combined with *da-Gal4, UAS-CycG$^{\Delta P}$* (filled circles) or not (empty circles) versus inter-individual variance (log10). Filled grey square: *+/da-Gal4, UAS-CycG$^{\Delta P}$*; empty grey square: *+/da-Gal4*. A strong positive correlation was observed between the two parameters (R= +0.67).

Figure 3: Candidate gene analyses – Genes encoding direct protein partners of Cyclin G located in deficiencies that modify *CycG$^{\Delta P}$*-induced FA.

In green, alleles that significantly increased *CycG$^{\Delta P}$*-induced FA**.** In orange, alleles that significantly decreased *CycG$^{\Delta P}$*-induced FA. In light grey, positive control *(+/da-Gal4, UAS-CycG$^{\Delta P}$*). In dark grey, alleles that did not modify *CycG$^{\Delta P}$*-induced FA. Several alleles were lethal (†) when combined to *+/da-Gal4* or *+/da-Gal4, UAS-CycG$^{\Delta P}$*.

*p<0.05, **p<0.01, ***p<0.001

Figure 4: Candidate gene analyses – Genes encoding members of the Hippo pathway (A), the InR/TOR pathway (B) and the Dpp and Wg morphogens (C).

In green, alleles that significantly increased *CycG$^{\Delta P}$*-induced FA**.** In grey, alleles that did not modify *CycG$^{\Delta P}$*-induced FA.

*p<0.05, **p<0.01, ***p<0.001

Supplementary Figure 1:

A - Position of the 15 landmarks on the wing. Landmarks 3 and 13 (red) were used to measure

305 wing length.
306 **B –** Diagrams of primary and secondary screens.
307 *Df*: deficiency; w^{n}: w^{5905} or w^{6326}; *Bal*: balancer chromosome; N: neutral deficiencies; D:
308 deficiency that decreased $CycG^{\Delta P}$-induced fluctuating asymmetry; E: deficiency that
309 increased $CycG^{\Delta P}$-induced fluctuating asymmetry.
310
311 **Supplementary Figure 2: Secondary screen – Mean wing size of flies heterozygous for**
312 **the deficiencies associated with *da-Gal4* (top) or *da-Gal4, UAS-CycG$^{\Delta P}$* (down).**
313 Box-plots showing mean wing size. In grey, mean wing size of *+/da-Gal4* (top) or *+/da-*
314 *Gal4, UAS-CycG$^{\Delta P}$* flies. In orange, mean wing size of deficiencies that decreased $CycG^{\Delta P}$-
315 induced FA combined with *da-Gal4* (top) or *da-Gal4, UAS-CycG$^{\Delta P}$* (down). In green, mean
316 wing size of deficiencies that increased $CycG^{\Delta P}$-induced FA combined with *da-Gal4* (top) *or*
317 *da-Gal4, UAS-CycG$^{\Delta P}$* (down).
318 The two red lines correspond to the mean wing size of *+/da-Gal4* (1161) and *+/da-Gal4, UAS-*
319 *CycG$^{\Delta P}$* (1014) flies.
320 *p<0.05, **p<0.01, ***p<0.001
321
322 **Table 1: Deficiencies modifying *CycG$^{\Delta P}$*-induced FA.**
323
324 **Supplementary Table 1: Deficiencies used in this study.**
325
326 **Supplementary Table 2: Alleles used in this study to identify genes that modify *CycG$^{\Delta P}$*-**
327 **induced fluctuating asymmetry.**
328
329 **Supplementary Table 3: Secondary screen for deficiencies which modify *CycG$^{\Delta P}$*-**
330 **induced FA.**
331
332 **REFERENCES**

333 1. Debat V. Mapping phenotypes: canalization, plasticity and developmental stability.
334 Trends Ecol Evol. 2001;16:555–61.

335 2. Leamy L, Klingenberg C, Sherratt E, Wolf J, Cheverud J. The Genetic Architecture of
336 Fluctuating Asymmetry of Mandible Size and Shape in a Population of Mice: Another
337 Look. Symmetry. 2015;7(1):146–63.

338 3. Takahashi KH, Okada Y, Teramura K, Tsujino M. Deficiency mapping of the genomic
339 regions associated with effects on developmental stability in Drosophila melanogaster.
340 Evolution. 2011;65:3565–77.

341 4. Takahashi KH, Okada Y, Teramura K. Genome-Wide Deficiency Mapping of the Regions
342 Responsible for Temporal Canalization of the Developmental Processes of Drosophila
343 melanogaster. J Hered. 2011;102(4):448–57.

344 5. Debat V, Bloyer S, Faradji F, Gidaszewski N, Navarro N, Orozco-Terwengel P, et al.
345 Developmental Stability: A Major Role for Cyclin G in Drosophila melanogaster. PLoS
346 Genet. 2011;7(10):e1002314.

347 6. Debat V, Peronnet F. Asymmetric flies: The control of developmental noise in Drosophila.
348 Fly Austin. 2013;7(2):1–8.

349 7. Carvalhal S, Ribeiro SA, Arocena M, Kasciukovic T, Temme A, Koehler K, et al. The
350 nucleoporin ALADIN regulates Aurora A localization to ensure robust mitotic spindle
351 formation. Zheng Y, editor. Mol Biol Cell. 2015 Oct;26(19):3424–38.

352 8. Dalton D, Chadwick R, McGinnis W. Expression and embryonic function of empty
353 spiracles: a Drosophila homeo box gene with two patterning functions on the anterior-
354 posterior axis of the embryo. Genes Dev. 1989 Dec 1;3(12a):1940–56.

355 9. Marygold SJ, Attrill H, Lasko P. The translation factors of Drosophila melanogaster. Fly
356 Austin. 2017;11(1):65–74.

357 10. Bettencourt-Dias M, Giet R, Sinka R, Mazumdar A, Lock WG, Balloux F, et al.
358 Genome-wide survey of protein kinases required for cell cycle progression. Nature.
359 2004;432(7020):980–7.

360 11. Grewal SS. Insulin/TOR signaling in growth and homeostasis: a view from the fly
361 world. Int J Biochem Cell Biol. 2009;41(5):1006–10.

362 12. Oughtred R, Rust J, Chang C, Breitkreutz B, Stark C, Willems A, et al. The BIOGRID
363 database: A comprehensive biomedical resource of curated protein, genetic, and
364 chemical interactions. Protein Sci. 2021 Jan;30(1):187–200.

365 13. Fischer P, Preiss A, Nagel AC. A triangular connection between Cyclin G, PP2A and
366 Akt1 in the regulation of growth and metabolism inDrosophila. Fly (Austin). 2016;1–8.

367 14. Tabata T, Takei Y. Morphogens, their identification and regulation. Development.
368 2004 Feb 15;131(4):703–12.

369 15. Srivastava D, Toledo M, Manchon L, Tazi J, Juge F. Modulation of Yorkie activity by
370 alternative splicing is required for developmental stability. EMBO J. (2021); 40:e104895

371 16. Dardalhon-Cuménal D, Deraze J, Dupont CA, Ribeiro V, Coléno-Costes A, Pouch J,
372 et al. Cyclin G and the Polycomb Repressive complexes PRC1 and PR-DUB cooperate
373 for developmental stability. PLoS Genet. 2018;14(7):e1007498.

374 17. Blagden SP, Gatt MK, Archambault V, Lada K, Ichihara K, Lilley KS, et al. Drosophila
375 Larp associates with poly(A)-binding protein and is required for male fertility and syncytial
376 embryo development. Dev Biol. 2009 Oct;334(1):186–97.

377 18. Deragon J, Bousquet-Antonelli C. The role of LARP1 in translation and beyond.
378 WIREs RNA. 2015 Jul;6(4):399–417.

379 19. Cockman E, Anderson P, Ivanov P. TOP mRNPs: Molecular Mechanisms and
380 Principles of Regulation. Biomolecules. 2020 Jun 27;10(7):969.

381 20. Berman AJ, Thoreen CC, Dedeic Z, Chettle J, Roux PP, Blagden SP. Controversies
382 around the function of LARP1. RNA Biol. 2021 Feb 1;18(2):207–17.

383 21. Zhang Y, Wang ZH, Liu Y, Chen Y, Sun N, Gucek M, et al. PINK1 Inhibits Local
384 Protein Synthesis to Limit Transmission of Deleterious Mitochondrial DNA Mutations. Mol
385 Cell. 2019 Mar;73(6):1127-1137.e5.

386

Figure 1

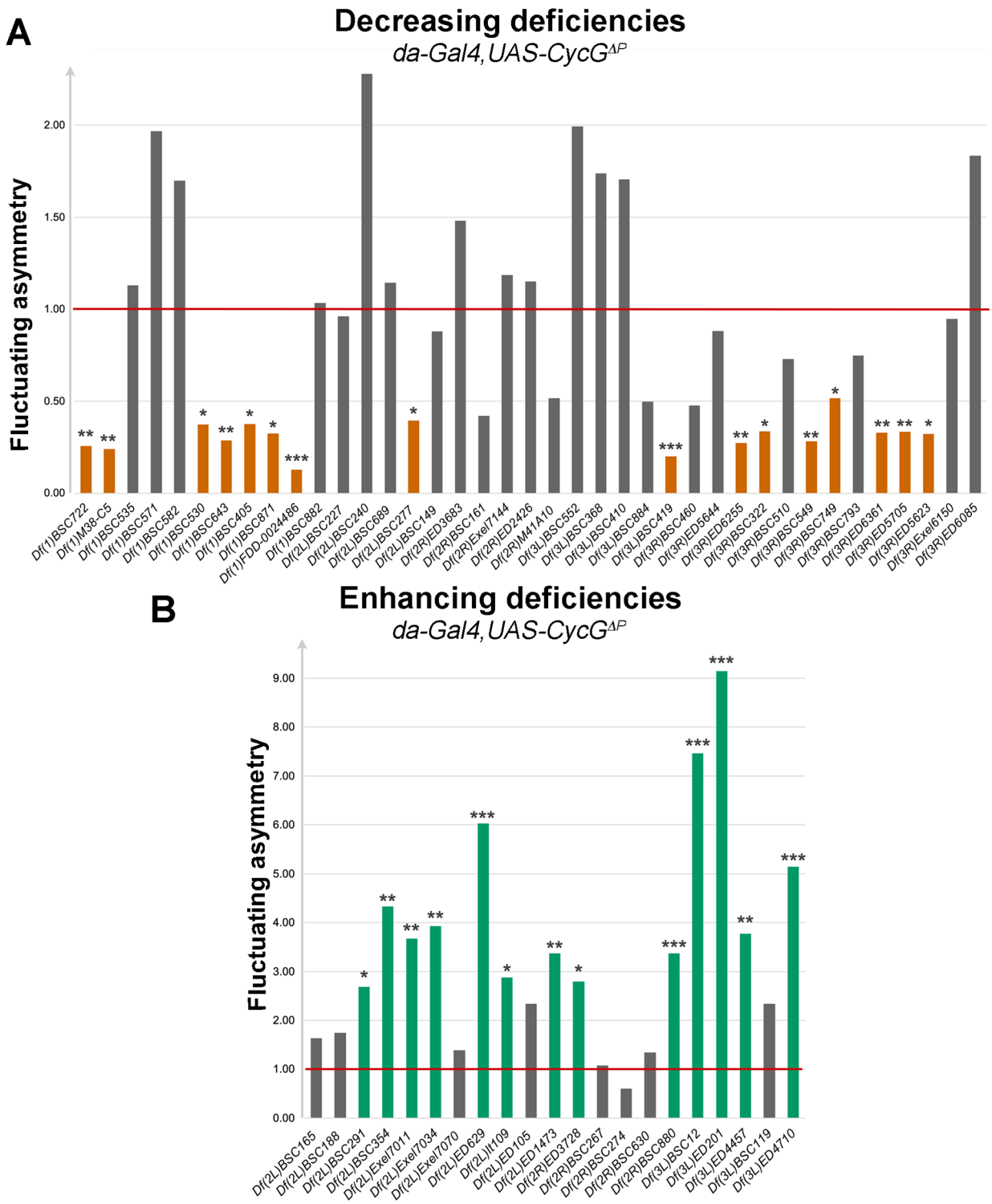
A
Decreasing deficiencies
da-Gal4,UAS-CycG^ΔP
Fluctuating asymmetry
0.00
0.50
1.00
1.50
2.00
Df(1)BSC722
Df(1)M38-C5
Df(1)BSC535
Df(1)BSC571
Df(1)BSC582
Df(1)BSC530
Df(1)BSC643
Df(1)BSC405
Df(1)BSC871
Df(1)FDD-0024486
Df(1)BSC882
Df(2L)BSC227
Df(2L)BSC240
Df(2L)BSC689
Df(2L)BSC277
Df(2L)BSC149
Df(2R)ED3683
Df(2R)BSC161
Df(2R)Exel7144
Df(2R)ED2426
Df(2R)M41A10
Df(3L)BSC552
Df(3L)BSC368
Df(3L)BSC410
Df(3L)BSC884
Df(3L)BSC419
Df(3R)BSC460
Df(3R)ED5644
Df(3R)ED6255
Df(3R)BSC322
Df(3R)BSC510
Df(3R)BSC549
Df(3R)BSC749
Df(3R)BSC793
Df(3R)ED6361
Df(3R)ED5705
Df(3R)ED5623
Df(3R)Exel6150
Df(3R)ED6085
B
Enhancing deficiencies
da-Gal4,UAS-CycG^ΔP
Fluctuating asymmetry
0.00
1.00
2.00
3.00
4.00
5.00
6.00
7.00
8.00
9.00
Df(2L)BSC165
Df(2L)BSC188
Df(2L)BSC291
Df(2L)BSC354
Df(2L)Exel7011
Df(2L)Exel7034
Df(2L)Exel7070
Df(2L)ED629
Df(2L)It109
Df(2L)ED105
Df(2R)ED1473
Df(2R)ED3728
Df(2R)BSC267
Df(2R)BSC274
Df(2R)BSC630
Df(2R)BSC880
Df(3L)BSC12
Df(3L)ED201
Df(3L)ED4457
Df(3L)BSC119
Df(3L)ED4710

Figure 2

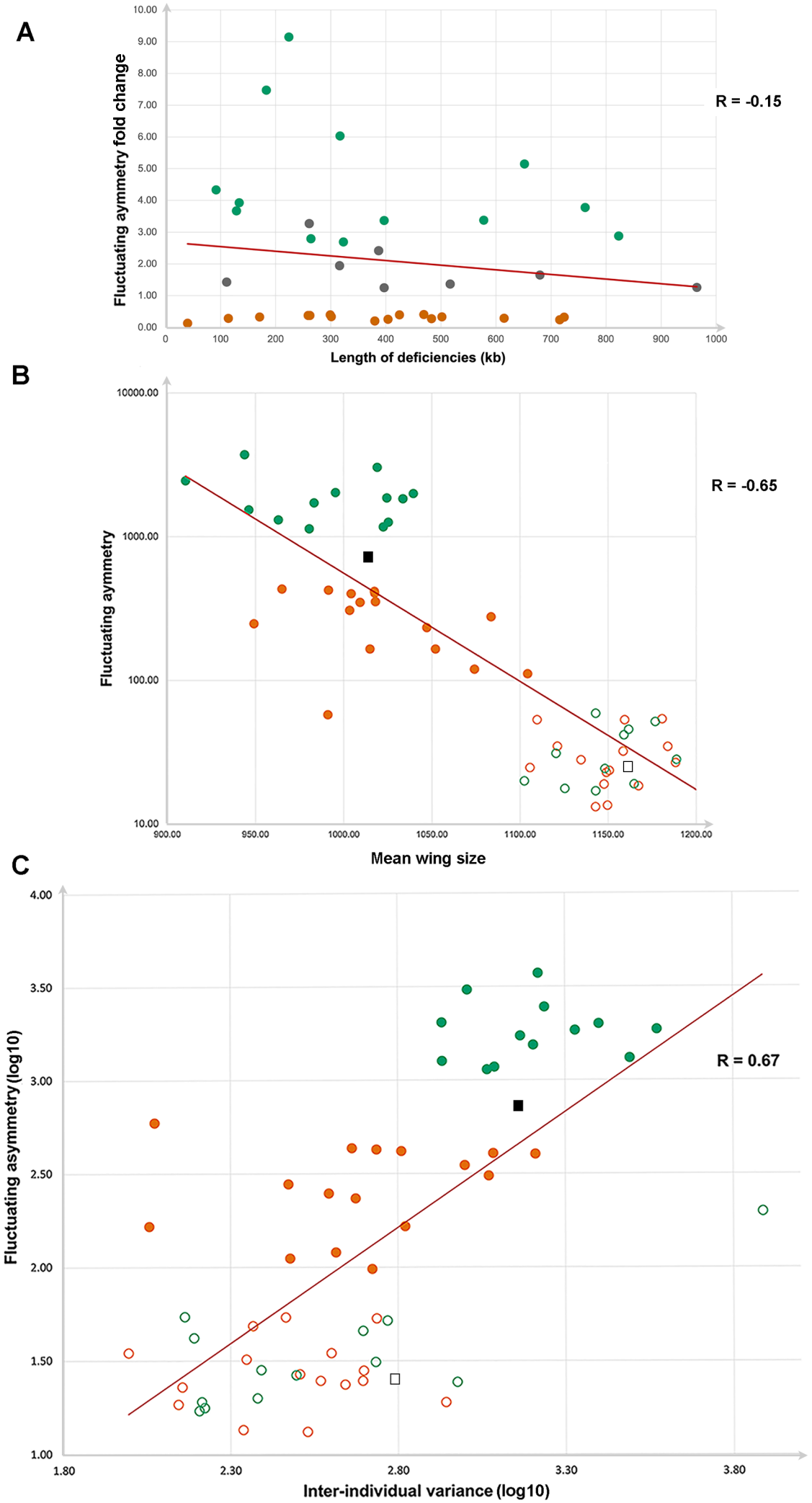
A
Fluctuating aymmetry fold change
Length of deficiencies (kb)
R = -0.15
B
Fluctuating aymmetry
Mean wing size
R = -0.65
C
Fluctuating asymmetry (log10)
Inter-individual variance (log10)
R = 0.67

Figure 3

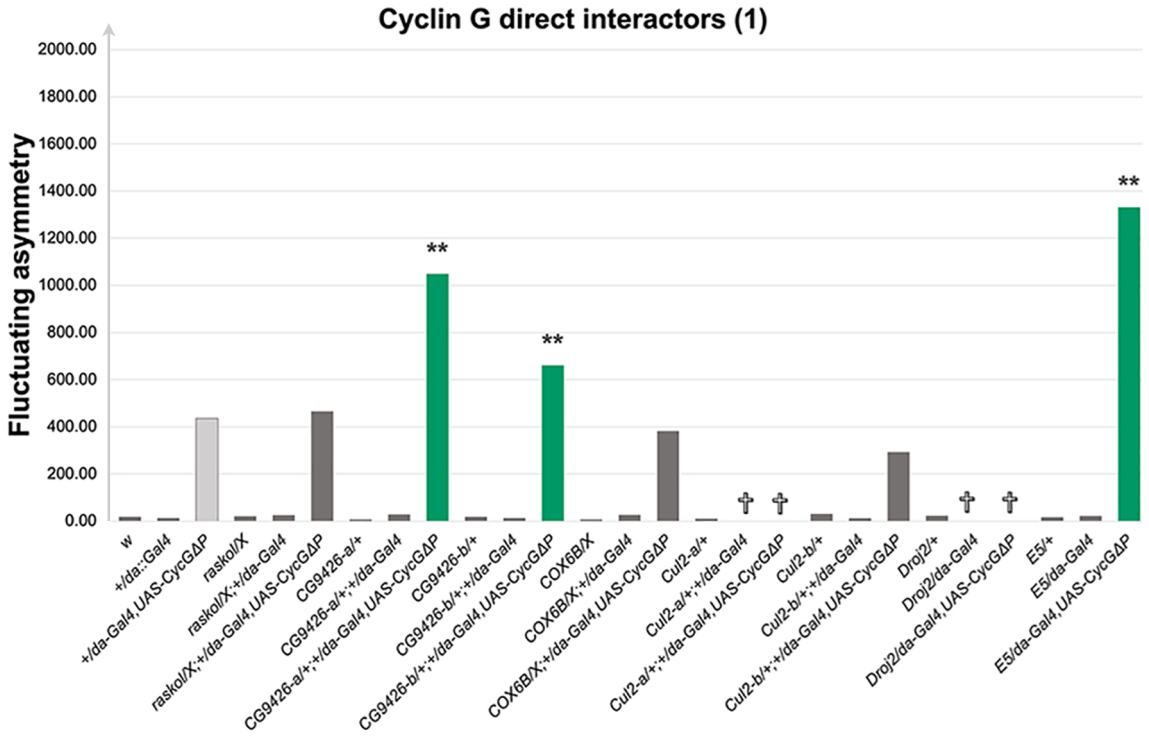
Cyclin G direct interactors (1)
Fluctuating asymmetry
2000.00
1800.00
1600.00
1400.00
1200.00
1000.00
800.00
600.00
400.00
200.00
0.00
**
**
**
w
+/da::Gal4
+/da-Gal4,UAS-CycGΔP
raskol/X
raskol/X;+/da-Gal4
raskol/X;+/da-Gal4,UAS-CycGΔP
CG9426-a/+
CG9426-a/+;+/da-Gal4
CG9426-a/+;+/da-Gal4,UAS-CycGΔP
CG9426-b/+
CG9426-b/+;+/da-Gal4
CG9426-b/+;+/da-Gal4,UAS-CycGΔP
COX6B/X
COX6B/X;+/da-Gal4
COX6B/X;+/da-Gal4,UAS-CycGΔP
Cul2-a/+
Cul2-a/+;+/da-Gal4
Cul2-a/+;+/da-Gal4,UAS-CycGΔP
Cul2-b/+
Cul2-b/+;+/da-Gal4
Cul2-b/+;+/da-Gal4,UAS-CycGΔP
Droj2/+
Droj2/da-Gal4
Droj2/da-Gal4,UAS-CycGΔP
E5/+
E5/da-Gal4
E5/da-Gal4,UAS-CycGΔP

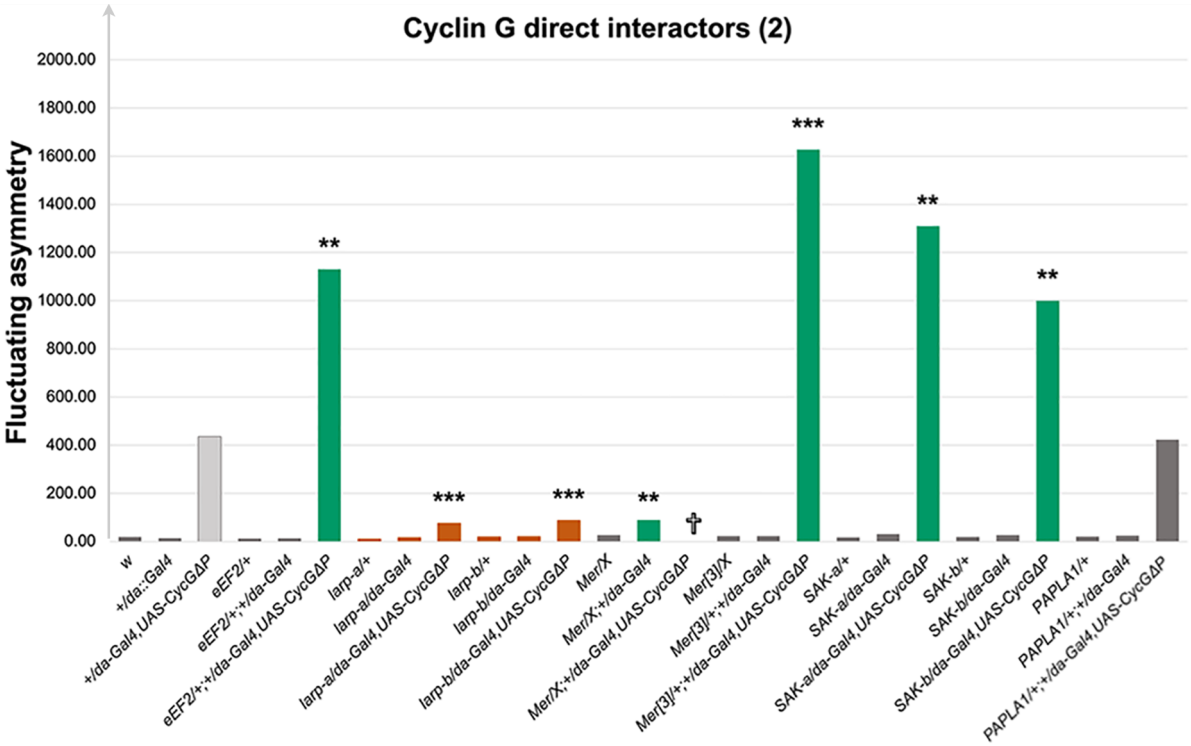
Cyclin G direct interactors (2)
Fluctuating asymmetry
2000.00
1800.00
1600.00
1400.00
1200.00
1000.00
800.00
600.00
400.00
200.00
0.00
**
***
***
**
***
**
**
w
+/da::Gal4
+/da-Gal4,UAS-CycGΔP
eEF2/+
eEF2/+;+/da-Gal4
eEF2/+;+/da-Gal4,UAS-CycGΔP
larp-a/+
larp-a/da-Gal4
larp-a/da-Gal4,UAS-CycGΔP
larp-b/+
larp-b/da-Gal4
larp-b/da-Gal4,UAS-CycGΔP
Mer/X
Mer/X;+/da-Gal4
Mer/X;+/da-Gal4,UAS-CycGΔP
Mer[3]/X
Mer[3]/+;+/da-Gal4
Mer[3]/+;+/da-Gal4,UAS-CycGΔP
SAK-a/+
SAK-a/da-Gal4
SAK-a/da-Gal4,UAS-CycGΔP
SAK-b/+
SAK-b/da-Gal4
SAK-b/da-Gal4,UAS-CycGΔP
PAPLA1/+
PAPLA1/+;+/da-Gal4
PAPLA1/+;+/da-Gal4,UAS-CycGΔP

Figure 4

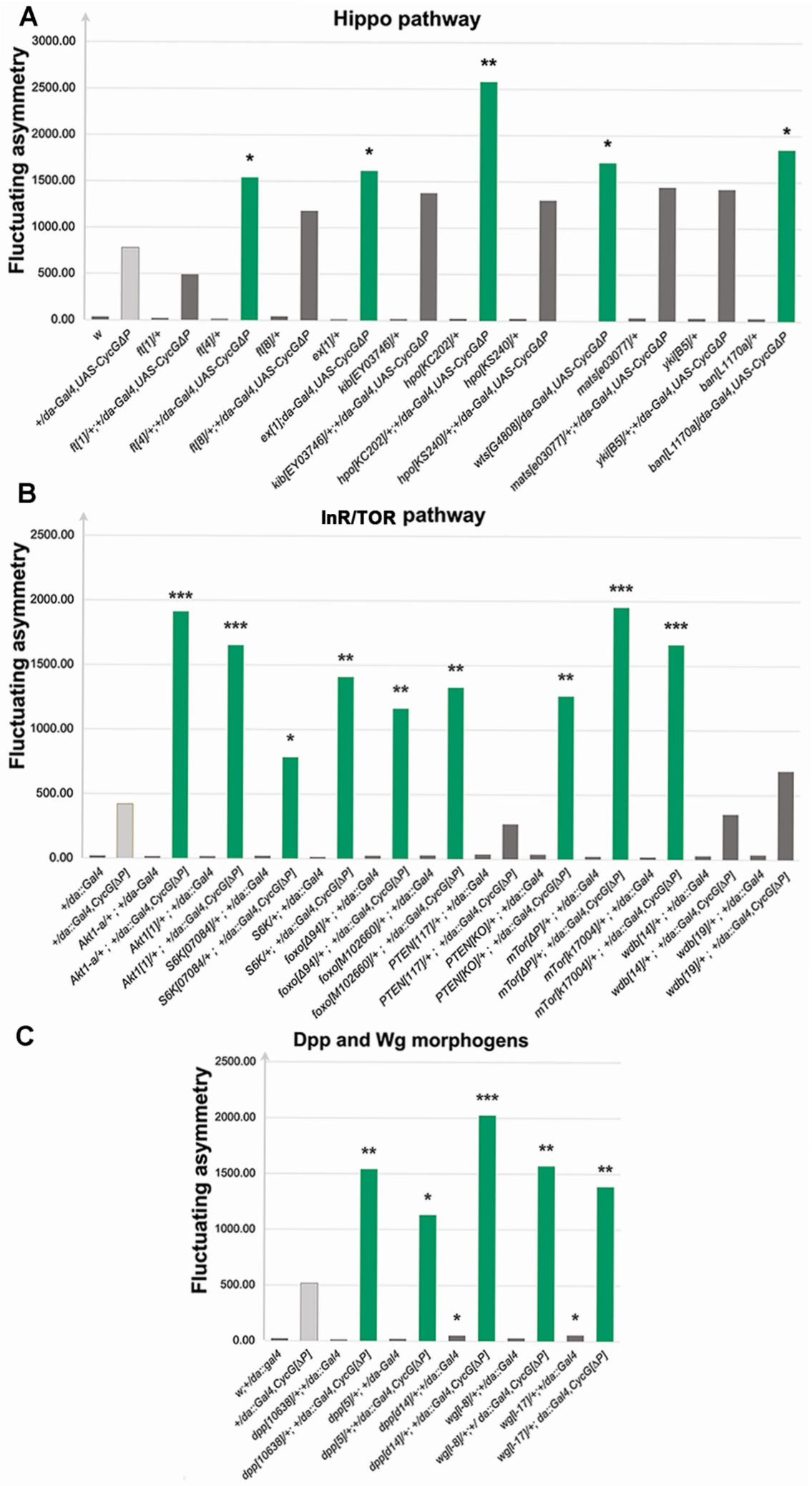
A
Hippo pathway
Fluctuating asymmetry
3000.00
2500.00
2000.00
1500.00
1000.00
500.00
0.00
w
+/da-Gal4,UAS-CycGΔP
ft[1]/+
ft[1]/+;+/da-Gal4,UAS-CycGΔP
ft[4]/+
ft[4]/+;+/da-Gal4,UAS-CycGΔP
ft[8]/+
ft[8]/+;+/da-Gal4,UAS-CycGΔP
ex[1]/+
ex[1];da-Gal4,UAS-CycGΔP
kib[EY03746]/+
kib[EY03746]/+;+/da-Gal4,UAS-CycGΔP
hpo[KC202]/+
hpo[KC202]/+;+/da-Gal4,UAS-CycGΔP
hpo[KS240]/+
hpo[KS240]/+;+/da-Gal4,UAS-CycGΔP
wts[G4808]/da-Gal4,UAS-CycGΔP
mats[e03077]/+
mats[e03077]/+;+/da-Gal4,UAS-CycGΔP
yki[B5]/+
yki[B5]/+;+/da-Gal4,UAS-CycGΔP
ban[L1170a]/+
ban[L1170a]/da-Gal4,UAS-CycGΔP
B
InR/TOR pathway
Fluctuating asymmetry
2500.00
2000.00
1500.00
1000.00
500.00
0.00
+/da::Gal4
+/da::Gal4,CycG[ΔP]
Akt1-a/+ ; +/da-Gal4
Akt1-a/+ ; +/da::Gal4,CycG[ΔP]
Akt1[1]/+ ; +/da::Gal4
Akt1[1]/+ ; +/da::Gal4,CycG[ΔP]
S6K[07084]/+ ; +/da::Gal4
S6K[07084/+ ; +/da::Gal4,CycG[ΔP]
S6K/+; +/da::Gal4
S6K/+; +/da::Gal4,CycG[ΔP]
foxo[Δ94]/+ ; +/da::Gal4
foxo[Δ94]/+ ; +/da::Gal4,CycG[ΔP]
foxo[M102660]/+ ; +/da::Gal4
foxo[M102660]/+ ; +/da::Gal4,CycG[ΔP]
PTEN[117]/+ ; +/da::Gal4
PTEN[117]/+ ; +/da::Gal4,CycG[ΔP]
PTEN[KO]/+ ; +/da::Gal4
PTEN[KO]/+ ; +/da::Gal4,CycG[ΔP]
mTor[ΔP]/+ ; +/da::Gal4
mTor[ΔP]/+ ; +/da::Gal4,CycG[ΔP]
mTor[k17004]/+ ; +/da::Gal4
mTor[k17004]/+ ; +/da::Gal4,CycG[ΔP]
wdb[14]/+ ; +/da::Gal4
wdb[14]/+ ; +/da::Gal4,CycG[ΔP]
wdb[19]/+ ; +/da::Gal4
wdb[19]/+ ; +/da::Gal4,CycG[ΔP]
C
Dpp and Wg morphogens
Fluctuating asymmetry
2500.00
2000.00
1500.00
1000.00
500.00
0.00
w;+/da::gal4
+/da::Gal4,CycG[ΔP]
dpp[10638]/+;+/da::Gal4
dpp[10638]/+; +/da::Gal4,CycG[ΔP]
dpp[5]/+; +/da-Gal4
dpp[5]/+;+/da::Gal4,CycG[ΔP]
dpp[d14]/+;+/da::Gal4
dpp[d14]/+; +/da::Gal4,CycG[ΔP]
wg[l-8]/+;+/ da::Gal4
wg[l-8]/+;+/ da::Gal4,CycG[ΔP]
wg[l-17]/+;+/da::Gal4
wg[l-17]/+; da::Gal4,CycG[ΔP]

Table 1: Deficiencies modifying *Cyclin G*-induced fluctuating asymmetry.
The fluctuating asymmetry fold-change corresponds to the ratio between fluctuating asymmetry of the deficiency combined to *da-Gal4,UAS-CycG*$^{\Delta P}$ and fluctuating asymmetry of *da-Gal4,UAS-CycG*$^{\Delta P}$.

Chromosome arm	Deficiency name	Cytological location	Fluctuating asymmetry fold-change	Adjusted p-value	Length (kb)
X	*Df(1)BSC530*	1A5;1B12	0.37329	4.68E-02	259
	Df(1)M38-C5	8B;8E	0.24024	2.86E-03	716
	Df(1)BSC722	10B3;10E1	0.25570	6.72E-03	404
	Df(1)FDD-0024486	14C4;14D1	0.12722	2.58E-06	40
	Df(1)BSC643	15F9;16F1	0.28609	7.33E-03	615
	Df(1)BSC405	16D5;16F6	0.37682	4.68E-02	262
	Df(1)BSC871	18D7;18F2	0.32513	2.55E-02	171
2L	*Df(2L)Exel7011*	22E1;22F3	3.67005	4.34E-03	129
	Df(2L)BSC354	26D7;26E3	4.32949	1.32E-03	92
	Df(2L)BSC291	27D6;27F2	2.69177	3.96E-02	323
	Df(2L)Exel7034	28E1;28F1	3.92670	2.69E-03	134
	Df(2L)ED629	29B4;29E4	6.02764	5.81E-05	317
	Df(2L)BSC277	34A1;34B2	0.39515	2.82E-02	425
	Df(2L)ED1473	39B4;40A5	3.37401	7.77E-03	578
	Df(2L)lt109	h35;h35	2.87894	2.34E-02	823
2R	*Df(2R)BSC880*	49A9;49E1	3.36810	9.85E-04	397
	Df(2R)ED3728	56D10;56E2	2.79286	2.50E-02	264
3L	*Df(3L)ED201*	61B1;61C1	9.14411	6.11E-07	224
	Df(3L)ED4457	67E2;68A7	3.77715	3.03E-03	762
	Df(3L)BSC12	69F6;70A2	7.46921	5.43E-06	183
	Df(3L)ED4710	74D1;75B11	5.14760	1.95E-04	652
	Df(3L)BSC419	78C2;78D8	0.20077	5.30E-04	380
3R	*Df(3R)BSC549*	83A6;83B6	0.28288	9.98E-03	114
	Df(3R)ED5623	87E3;88A4	0.32086	1.65E-02	724
	Df(3R)ED5705	88E12;89A5	0.33282	1.69E-02	502
	Df(3R)ED6255	97D2;97F1	0.27386	5.53E-03	483
	Df(3R)BSC322	98C3;98D7	0.33719	3.21E-02	301
	Df(3R)BSC749	100B1;100C1	0.39540	9.04E-03	299
	Df3R)ED6361	100C7;100E3	0.40559	1.17E-02	469